

Enhancement of Power Quality of PMSG Based DG Set Using Fuzzy Logic Controller

E. Sasi Kumar Naik¹, Dr. K. Jithendra Gowd²

¹ PG Scholar, Department of Electrical Engineering, JNTUA College of Engineering, Anantapur, Andhra Pradesh, India

² Assistant Professor, Department of Electrical Engineering, JNTUA College of Engineering, Anantapur, Andhra Pradesh, India

ABSTRACT

Permanent Magnet Synchronous Generator (PMSG) is having potential application in isolated supply systems. This paper presents power quality improvement of PMSG based DG (Diesel Generator) set nourishing three-stage loads utilizing STATCOM (Static Compensator) with Fuzzy Controller. Here we are utilizing the Fuzzy controller contrasted with different controllers i.e. The Fuzzy Controller is the most reasonable basic component, giving the operation of an electronic framework with choices of specialists. A 3-leg VSC (Voltage Source Converter) with a capacitor on the DC interface is utilized as STATCOM. The reference source currents for the framework are evaluated utilizing an Adaline based control Algorithm. A PWM (Pulse Width Modulation) current controller is utilizing for era of gating pulses of IGBTs (Insulated Gate Bipolar Transistors) of three leg VSC of the STATCOM. The STATCOM is used for voltage control, harmonics elimination, power factor improvement, load balancing and load compensation. The performance of the system is experimentally tested on various types of loads under steady state and dynamic conditions. A 3-stage induction engine with variable frequency drive is utilized as a model of diesel motor with the speed control. Along with these, the DG set runs at constant speed with the goal that the frequency of supply is constant independent of loading condition.

Keywords : PMSG, STATCOM, IGBT, VSC, PWM, Fuzzy Controller.

I. INTRODUCTION

PMSGs have picked up fame as of now on account of their potential use in WECS (Wind Energy Conversion Systems) [1-4]. The progression in the field of uncommon earth changeless magnet with high field force, for example, neodymium-iron-boron (Nd-Fe-B) has additionally demonstrated incredible open doors in the field of vehicle industry [5-7]. These generators offer many advantages over wound field type synchronous generators such as brushless operation, no rotor winding, small size, no rotor copper losses, less maintenance and high efficiency. In light of these focal points PMSGs are additionally being utilized as a part of turbofan jet motor electrical power era [8]. The fundamental difficulties in PMSG are voltage and frequency control under fluctuating load conditions. These difficulties can be effectively cleared with the use of control converters. In WECS, the voltage and frequency of PMSG can be controlled utilizing AC-DC-AC control converters [9,10]. PMSG is compact in size so these generators have potential applications in DG

(Diesel Generator) set based separated supply frameworks. The diesel generator sets are kept running at a consistent speed with the diesel motor as a prime mover. There is no issue of frequency control in these supply frameworks. The primary assignment in DG sets based supply frameworks is to keep up the steady terminal voltage. There are consistent efforts of researchers to develop methods to improve voltage regulation of PMSG based isolated supply systems. Suitable design of rotor with Nd-Fe-B magnet can reduce the voltage regulation of PMSG. Chan et. al. [11] exhibited the investigation of PMSG with Nd-Fe-B permanent magnet rotor nourishing resistive load to accomplish zero voltage regulation. They have exhibited that the opposite saliency impact of PMSG helps in change of voltage control of the generator. Chen et. al. [12] has detailed utilization of fixed capacitor for helping excitation of PMSG to enhance the voltage control of the generator. Rahman et.al. [13] have regulated the terminal voltage of diesel motor drive PMSG for detached supply framework utilizing fixed capacitor-thyristor controlled reactor. Errami et.al. [14]

have proposed variable structure coordinate torque control method for PMSG based WECS. In the research work at DG sets, almost no consideration has been paid to potential utilization of PMSG in DG sets independent supply frameworks. The voltage of PMSG based DG set in secluded supply frameworks can be controlled utilizing STATCOM (Static Compensator). STATCOM is generally utilized as a part of framework associated with secluded supply frameworks such for voltage and frequency control [15-21]. What's more, it can be utilized for load adjusting, load pay and receptive power compensation. In the proposed framework with PMSG driven by diesel motor, STATCOM is utilized for voltage control of the PMSG. Many control algorithms are accessible for era of reference source currents. Proposed framework utilizes an Adaline based control calculation in light of its straight forwardness and appropriateness under changing burden conditions [22].

II. SYSTEM CONFIGURATION

The proposed system consisting of a PMSG based DG set, a three leg VSC, and linear/nonlinear loads, is shown in Fig. 1. A RC filter is used for filtering high frequency ripple from voltage at PCC (Point of Common Coupling). A 3-leg VSC is used a STATCOM. The VSC is connected to PCC through three interfacing inductors. The interfacing inductors connected between three legs of VSC and PCC are used to filter the high frequency ripples from current. The proposed system uses a specially designed PMSM of 3.7 kW, 50 Hz, 4-pole, 230 V. The values of interfacing inductors, components of RC filter, DC link capacitor and detailed data of PMSG are given in Appendix.

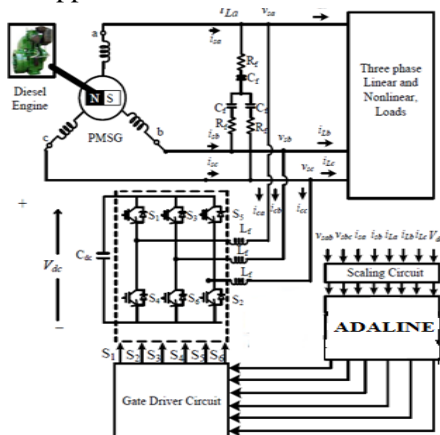


Figure1. Configuration of PMSG based DG set feeding three phase loads

III. CONTROL ALGORITHM

Adaline based control algorithm used in the proposed system for estimation of reference source currents is demonstrated in Fig.2. The Adaline based control algorithm estimates amplitude of fundamental components of active and reactive components of load currents. It uses a fixed step size which may have any value from 0.1 to 1 for fast convergence. In-phase and quadrature phase unit templates are used for estimation of reference source currents.

A. Extraction of Quadrature Phase and In-Phase Unit Templates

In-phase unit templates are extracted by dividing instantaneous phase-voltages by amplitude of phase voltages (V_t) as,

$$u_{ap} = v_{sa}/V_t, u_{bp} = v_{sb}/V_t, u_{cp} = v_{sc}/V_t \quad (1)$$

Where v_{sa} , v_{sb} and v_{sc} are instantaneous phase-voltages which are obtained from sensed lined voltage obtained as [19].

$$\begin{pmatrix} v_{sa} \\ v_{sb} \\ v_{sc} \end{pmatrix} = \frac{1}{3} \begin{bmatrix} 2 & 1 \\ -1 & 1 \\ -1 & -2 \end{bmatrix} \begin{bmatrix} v_{sab} \\ v_{sbc} \end{bmatrix} \quad (2)$$

The amplitude of phase voltages is obtained from instantaneous phase voltages as [19],

$$V_t = \sqrt{\frac{2}{3}(v_{sa}^2 + v_{sb}^2 + v_{sc}^2)} \quad (3)$$

The quadrature unit templates are extracted using in-phase unit templates as,

$$u_{aq} = (-u_{bq} + u_{cq})/\sqrt{3} \quad (4)$$

$$u_{bq} = (3u_{aq} + u_{bq} - u_{cq})/2\sqrt{3} \quad (5)$$

$$u_{cq} = (3u_{ap} + u_{bp} - u_{cp})/2\sqrt{3} \quad (6)$$

B. Estimation of Active Power Component of Reference Source Current

The Adaline limits the mistake between real load current and its evaluated weight by improving the weights of dynamic and reactive parts of load streams.

The weight vector for dynamic part of load current of each stage is communicated as [22],

$$W_p(n) = W_p(n-1) + \mu^* \{i_L(n) - \{W_p(n) \times u_p(n)\}\} * u_p(n) \quad (7)$$

Where, μ is fixed step size having any value from 0.1 to 1. Here the step size in proposed system is taken to be 0.2.

For a three phase system, the weight of active component of load current is given as,

$$W_p(n) = \frac{W_{ap}(n) + W_{bp}(n) + W_{cp}(n)}{3} \quad (8)$$

where $W_{ap}(n)$, $W_{bp}(n)$ and $W_{cp}(n)$ are weights corresponding to active components of load currents in phase 'a', phase 'b' and phase 'c' respectively.

The weight of active power component of reference source current is obtained by adding weight vectors of (8) to the weight obtained from the output of DC link voltage PI (Proportional-Integral) controller. The input to DC link PI controller is an error voltage given as,

$$V_{dcr}(n) = V_{dcref}(n) - V_{dc}(n) \quad (9)$$

Where, $V_{dc}(n)$ is sensed voltage on DC link voltage and $V_{dcref}(n)$ is reference voltage of the DC link.

The output of the PI controller of DC link can be given as,

$$W_{qSTAT}(n) = W_{qSTAT}(n-1) + k_{pdc} \{V_{dcr}(n) - V_{dcr}(n-1)\} + k_{idc} V_{dcr}(n) \quad (10)$$

Where, $k_{pdc}=0.3$ and $k_{idc}=0$ are proportional and integral gain parameters of the PI controller of DC link[23].

The final estimated weight of the amplitude of active power component of reference source current is given as,

$$W_{pT}(n) = W_{qSTAT}(n-1) + W_p(n) \quad (11)$$

The instantaneous active components of 3-phase reference source currents are obtained by multiplying weight vector of active power component and in-phase unit templates as under,

$$i_{sap}^*(n) = W_{pT}(n) * u_{ap}(n) \quad (12)$$

$$i_{sbp}^*(n) = W_{pT}(n) * u_{bp}(n) \quad (13)$$

$$i_{scp}^*(n) = W_{pT}(n) * u_{cp}(n) \quad (14)$$

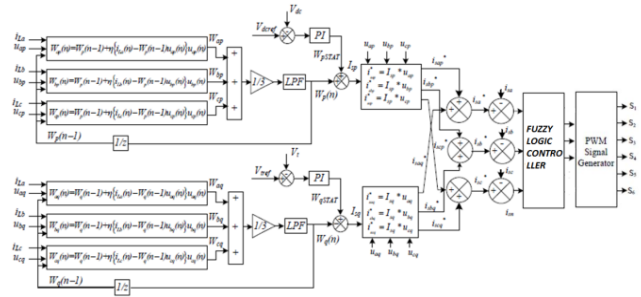


Figure 2. Adaline based control algorithm for PMSG Based DG set feeding three-phase loads

C. Estimation of Reactive Power Component of Reference Source Current

The weight vector for reactive power component of load current of each phase is given as,

$$W_q(n) = W_q(n-1) + \mu^* \{i_L(n) - \{W_{qT}(n) \times u_q(n)\}\} * u_q(n) \quad (15)$$

Final weight of reactive component of load current is given as,

$$W_q(n) = \frac{W_{aq}(n) + W_{bq}(n) + W_{cq}(n)}{3} \quad (16)$$

where $W_{aq}(n)$, $W_{bq}(n)$ and $W_{cq}(n)$ are weights corresponding to the reactive components of load currents in phase 'a', phase 'b' and phase 'c' respectively.

The output of terminal voltage PI controller is considered weight of receptive power part of STATCOM current. The yield of the terminal voltage PI controller is given as,

$$W_{qSTAT}(n) = W_{qSTAT}(n-1) + k_{pv} \{V_e(n) - V_e(n-1)\} + k_{iv} V_e(n) \quad (17)$$

Where, $k_{pv}=1.5$ and $k_{iv}=0.1$ are gain parameters of terminal voltage PI controller [23], and $V_e(n)$ is error voltage. The error voltage is computed as,

$$V_e(n) = V_{tref}(n) - V_t(n) \quad (18)$$

Where, $V_{tref}(n)$ is amplitude of reference terminal phase voltage and $V_t(n)$ is the amplitude of instantaneous phase voltage at PCC.

The weight of reactive segment of load current is subtracted from the output of terminal voltage PI controller to get the weight vector of reference source current as,

$$W_{qT}(n) = W_{qSTAT}(n-1) + W_q(n) \quad (19)$$

The instantaneous reactive components of three phase reference source currents are obtained weight of reference source current and quadrature phase unit templates as,

$$i_{saq}^*(n) = W_{qT}(n) * u_{aq}(n) \quad (20)$$

$$i_{sbq}^*(n) = W_{qT}(n) * u_{bq}(n) \quad (21)$$

$$i_{scq}^*(n) = W_{qT}(n) * u_{cq}(n) \quad (22)$$

D. Estimation of Reference Source Currents

The instantaneous reference source currents are acquired by including instantaneous active and reactive power parts of reference source currents as under,

$$\begin{aligned} i_{sa}^* &= i_{sap}^* + i_{saq}^*; i_{sb}^* = i_{sbp}^* + i_{sbq}^*; \\ i_{sc}^* &= i_{scp}^* + i_{scq}^* \end{aligned} \quad (23)$$

The estimated reference source currents and sensed source currents are compared with each other using Fuzzy Logic Controller and error is given to the PWM current controller to generate gating pulses for IGBTs of VSC of STATCOM.

IV. FUZZY LOGIC CONTROLLER

Fuzzy Logic Controller is one of the most successful applications of fuzzy set theory. Its major features are the use of linguistic variables rather than numerical variables. The basic structure of the FLC is shown in Fig 3.

The fuzzifier converts input data into suitable linguistic values by using fuzzy sets. The fuzzy sets are introduced with membership functions like triangle, sigmoid, trapezoid. The knowledge base consists of a data base with necessary linguistic definitions and control rule set. The rule set of knowledge base consists of some fuzzy rules that define the relations between inputs and outputs. Inference engine simulates the human decision process. This unit infers the fuzzy control action from the knowledge of the control rules and the linguistic variable definitions. Therefore, the knowledge base and the inference engine are in interconnection during the control process.

Firstly active rules are detected by substituting fuzzified input variables into rule base. Then these rules are combined by using one of the fuzzy reasoning methods.

Max-Min and Max-Product are most common fuzzy reasoning methods. The defuzzifier converts the fuzzy control action that infers from inference engine to a non fuzzy control action.

Different defuzzification methods are used such as center of gravity, mean of maxima and min-max weighted average formula. Center of gravity is the most common defuzzification method shown in Eq (24)

$$Z^* = \frac{\sum \mu(z) \cdot z}{\sum \mu(z)} \quad (24)$$

Where $\mu(z)$ is the grade of membership, z is the output of each rules and z^* is the defuzzified output.

The first important step in the fuzzy controller definition is the choice of the input and output variables. In this study, the output voltage error and its rate of change are defined as input variables and change in duty cycle is the controller output variable. The three variables of the FLC are the error, the change in error and the change in output and FLC is having seven triangle membership functions for each variable. The basic fuzzy sets of membership functions for the variables are as shown in the Figs. 3a, 3b and 3c.

The fuzzy sets are expressed by linguistic variables positive large (PL), positive medium (PM), positive small (PS), zero (Z), negative small (NS), negative medium (NM), negative large (NL), for all three variables. A rule in the rule base can be expressed in the form: If (e is NL) and (de is NL), then (co is NL). The rules are set based upon the knowledge of the system and the working of the system. The number of rules can be set as desired. The numbers of rules are 49 for the seven membership functions of the error and the change in error (inputs of the FLC).

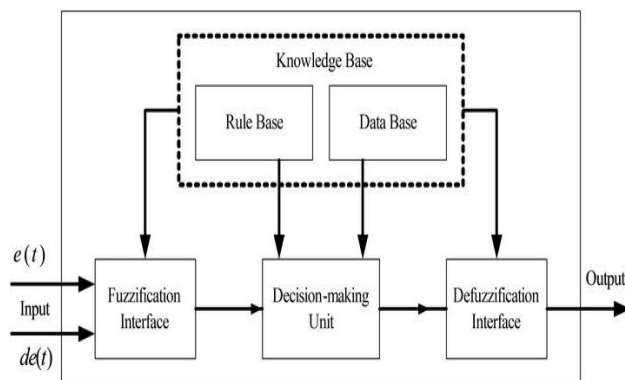


Figure3. Fuzzy logic controller

V. RESULTS AND DISCUSSION

A. Performance of DG System under Linear Loads

The performance of the PMSG based DG set under linear load using Fuzzy Controller is demonstrated in Fig. 4. The system is subjected to three phase load of 2.62 kW at displacement power factor of 0.99. Fig. 4(a) demonstrates the source voltages (v_{sab}) and source currents (i_{sa} , i_{sb} , i_{sc}). Fig. 4(b) shows the source voltage (v_{sab}) and load currents (i_{La} , i_{Lb} , i_{Lc}). Fig.4(c) demonstrates the source voltage (v_{sab}) and STATCOM currents (i_{Ca} , i_{Cb} , i_{Cc}). Figs.4(d-i) shows the active and reactive powers of source,load and STATCOM respectively.It is observed from the waveforms that the Controller is able to maintain the terminal voltage almost at 220 V under a load of 2.62 kW.

The dynamic performance of the system under the transient condition using Fuzzy Controller is demonstrated in Fig. 5.The system is subjected to three phase load of 3.16 kW at displacement power factor of 0.90. Initially, the system is subjected to unbalanced load by removing the load from phase 'c'. The dynamic performance of system is tested by changing the load from unbalanced to balanced by inserting the load in phase 'c'. It can be observed from the waveforms that system is able to overcome the transient within couple of cycles.

B. Performance of DG System under Nonlinear Loads

The performance of the system under nonlinear load using Fuzzy Controller is demonstrated in Fig.6. The system is subjected to a balanced nonlinear load of 2.99 kW. Fig. 6(a) shows the source voltages (v_{sab}) and source currents (i_{sa} , i_{sb} , i_{sc}). Fig.6(b) shows the source voltage (v_{sab}) and load currents (i_{La} , i_{Lb} , i_{Lc}). Fig.6(c) shows the source voltage (v_{sab}) and STATCOM current (i_{Ca} , i_{Cb} , i_{Cc}). Figs.6(d-i) shows active and reactive powers of source, load and STATCOM. Figs. 6(j)-(l) shows the THDs of the source voltage, source current and load current. The load currents are distorted with THD of 10.47 %, the source current has THD of 0.50%. The source terminal voltage has a THD of 0.13 %.

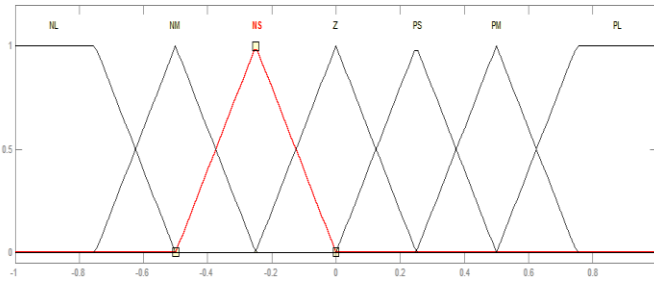


Figure3a. Membership functions of error

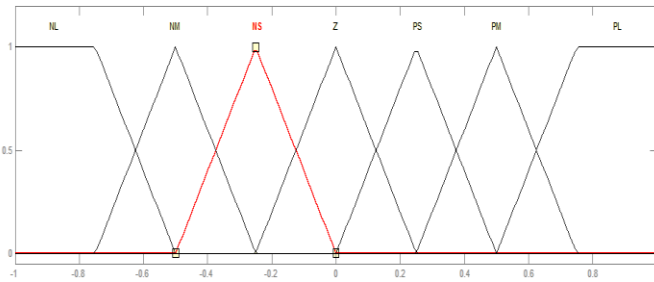


Figure3b. Membership functions of change in error

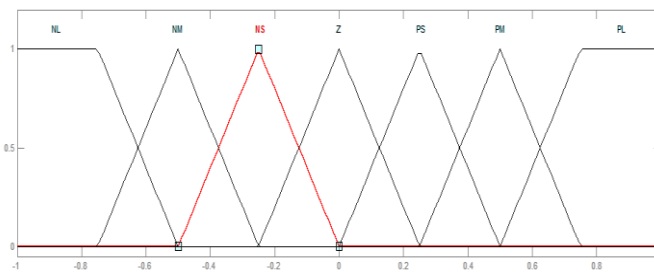
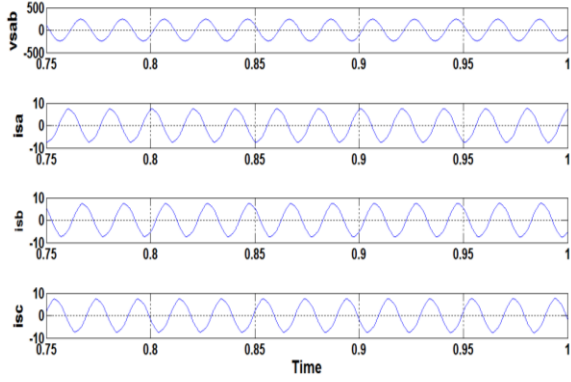


Figure3c. Membership functions of controlled output

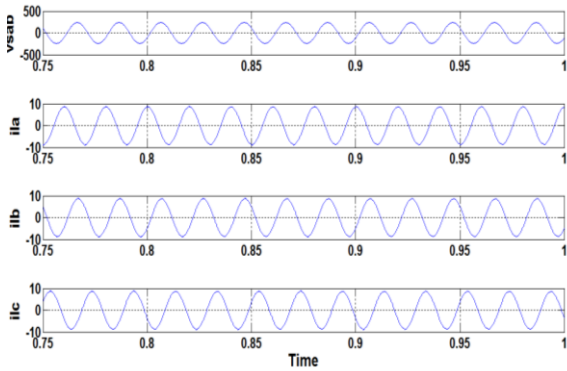
TABLE-1: Rule Base of Fuzzy Logic Controller

$e/\Delta e$	NL	NM	NS	Z	PS	PM	PL
NL	NL	NL	NL	NL	NM	NS	Z
NM	NL	NL	NL	NM	NS	Z	PS
NS	NL	NL	NM	NS	Z	PS	PM
Z	NL	NM	NS	Z	PS	PM	PL
PS	NM	NS	Z	PS	PM	PL	PL
PM	NS	Z	PS	PM	PL	PL	PL
PL	Z	PS	PM	PL	PL	PL	PL

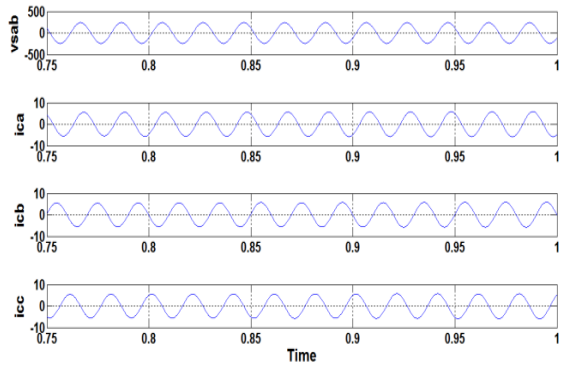
VI. SIMULATION RESULTS



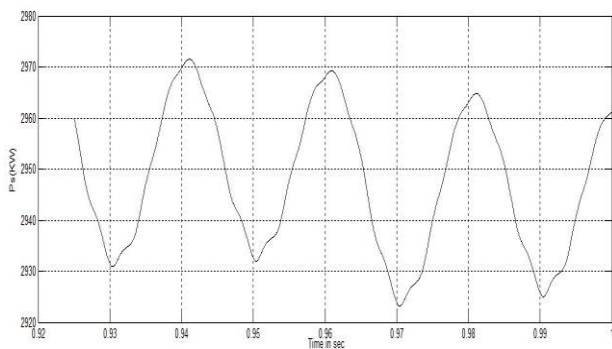
(a)



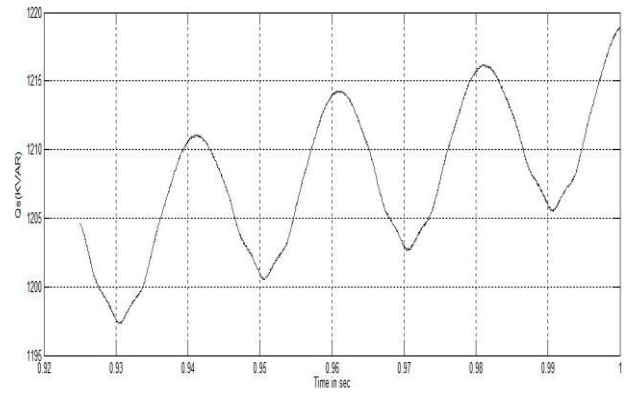
(b)



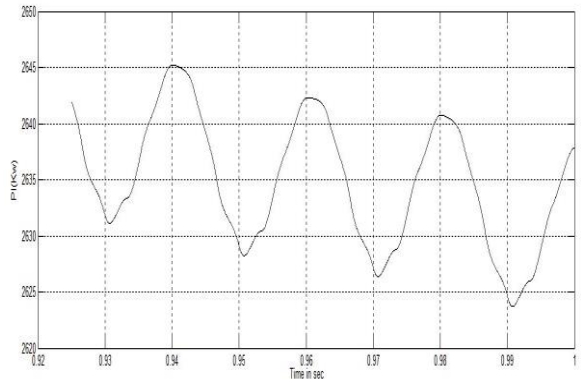
(c)



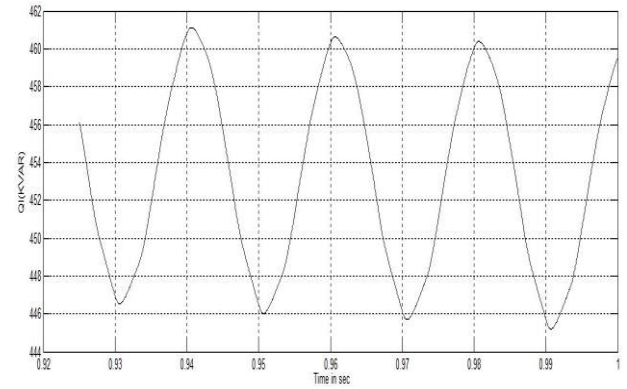
(d)



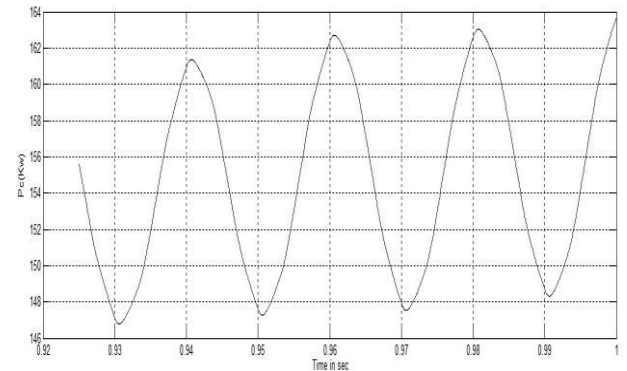
(e)



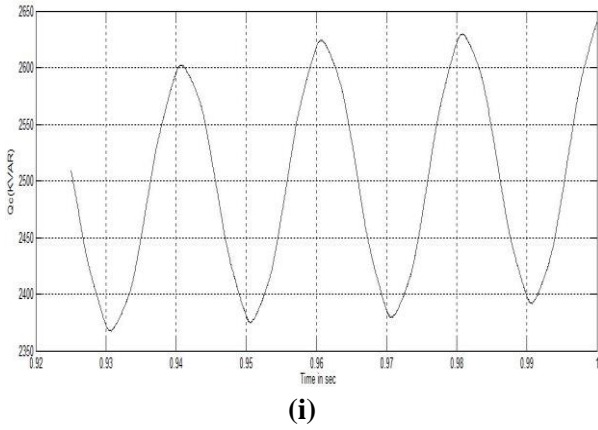
(f)



(g)



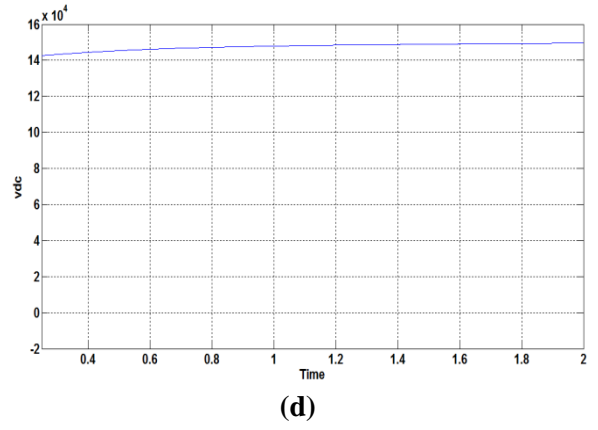
(h)



(i)

Figure 4. Performance under balanced linear loads

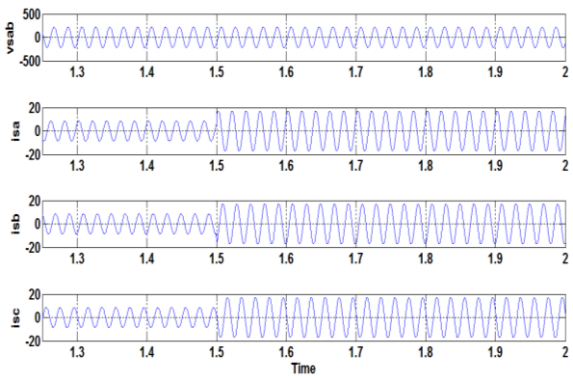
- (a) v_{sab} and i_{sabc} (b) v_{sab} and i_{Labc} (c) v_{sab} and i_{cabc}
 (d) P_s , (e) Q_s , (f) P_L , (g) Q_L , (h) P_C , (i) Q_C



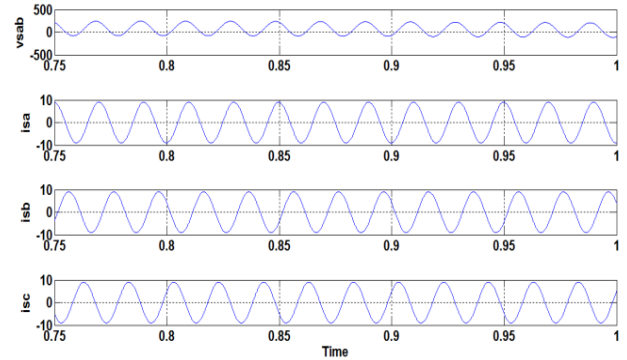
(d)

Figure 5. Dynamic performance at linear loads

- (a) v_{sab} , i_{sa} , i_{sb} and i_{sc} , (b) v_{sab} , i_{La} , i_{Lb} and i_{Lc} (c) V_{dc} , i_{sa} , i_{La} and i_{Ca}
 (d) V_{dc}



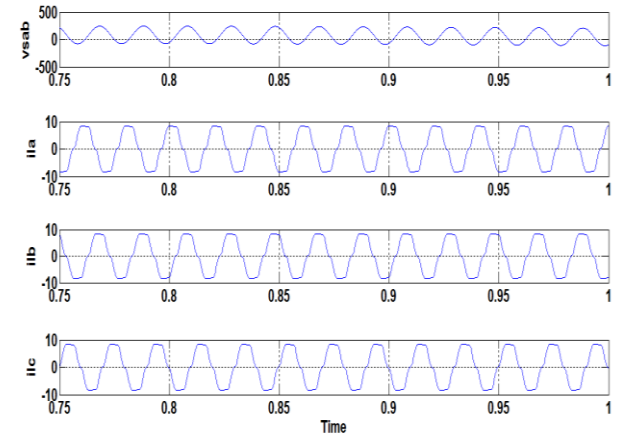
(a)



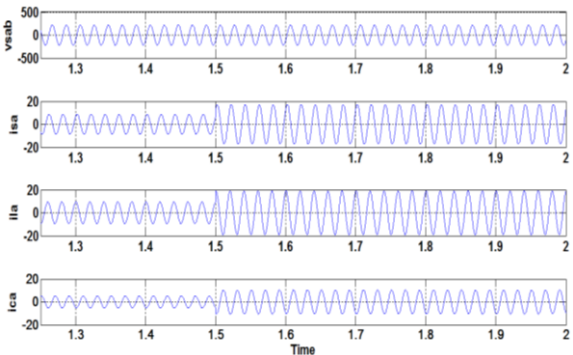
(a)



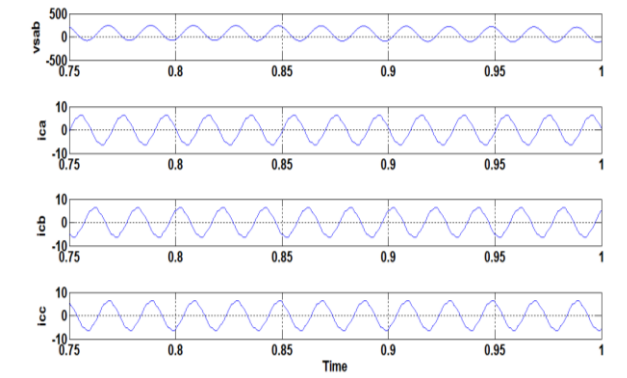
(b)



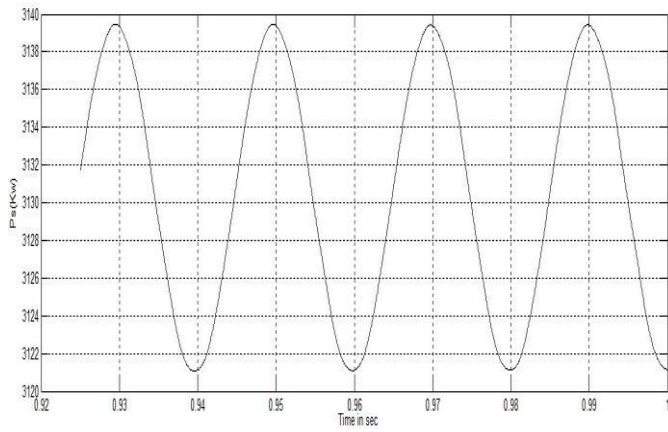
(b)



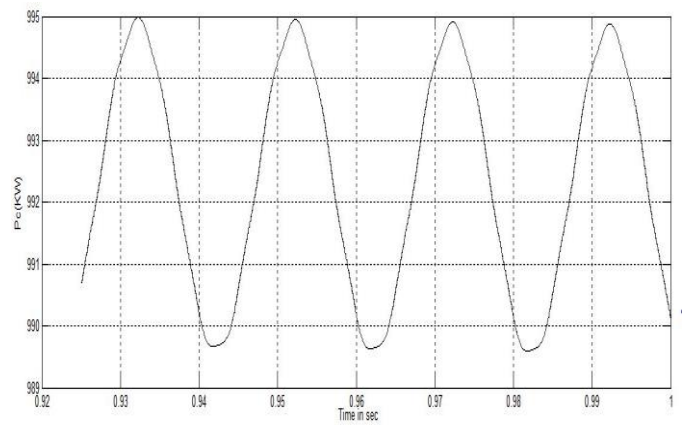
(c)



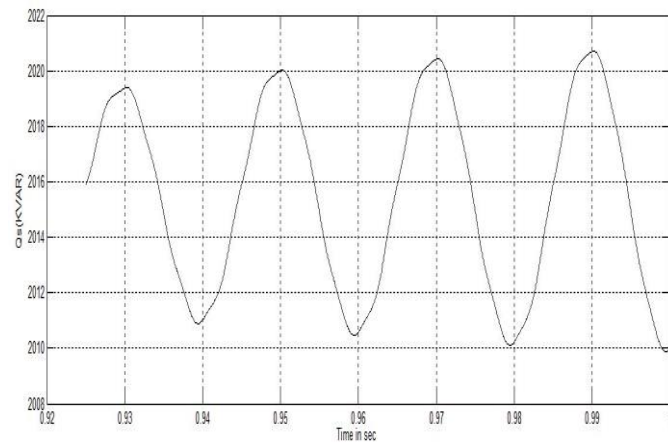
(c)



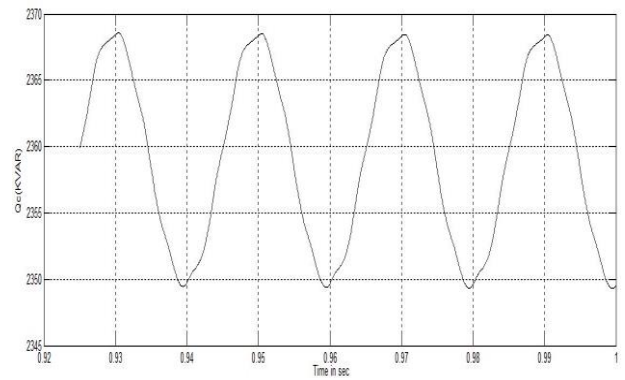
(d)



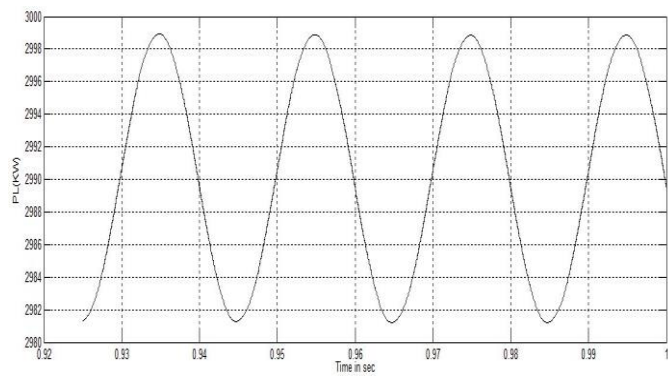
(h)



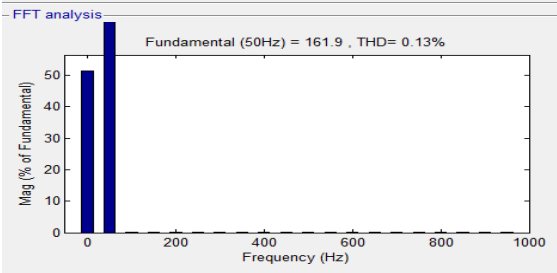
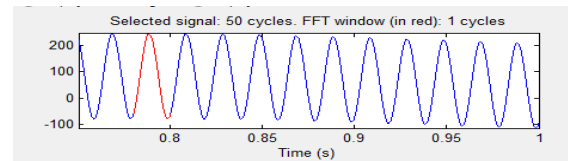
(e)



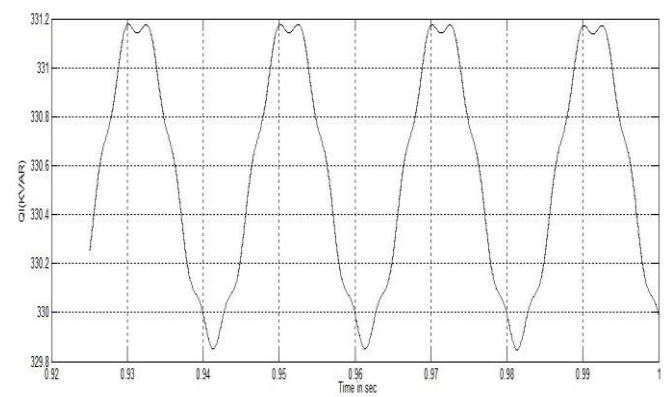
(i)



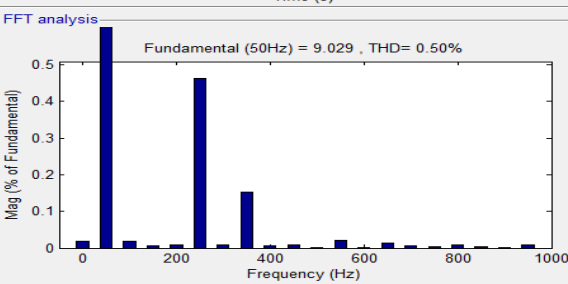
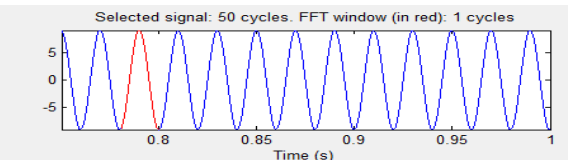
(f)



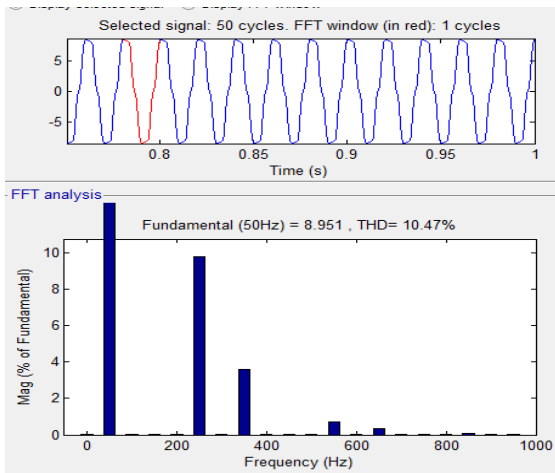
(j)



(g)



(k)



(l)

Figure 6. Performance under balanced nonlinear loads

- (a) v_{sab} and i_{sabc} (b) v_{sab} and i_{labc} (c) v_{sab} and i_{cabc}
 (d) P_s , (e) Q_s , (f) PL , (g) QL , (h) P_c , (i) Q_c , (j) THD of v_{sab}
 (k) THD of i_{sa} (l) THD of i_{La}

Table-2: THD COMPARISSION

Parametr	PI Controller	FLC
%THD of V_{sab}	2.84	0.13
%THD of i_{sa}	2.91	0.50
%THD of i_{La}	21.53	10.47

VII. APPENDIX

PMSG	3.7Kw,230V,3phase,starconnected,1500rpm,50Hz, $X_d=4.669\Omega$, $X_q=5.573\Omega$, $R_s=0.2747\Omega$
STATCOM	$R_f=5\Omega$, $C_f=5.25\mu F$, $L_f=3.5mH$, $C_{dc}=1650\mu F$
PI controller	$K_{pv}=1.5$, $k_{iv}=0.1$, $k_{pdc}=0.3$, $k_{idc}=0$

VIII. CONCLUSIONS

STATCOM has been used for power quality improvement of the PMSG based DG set for voltage control, harmonic elimination, and load adjustment. Additionally it has been found that the STATCOM is able to maintain source streams when the load is profoundly unequal because of expulsion of load from phase 'c'. The proposed system is a steady speed DG set so there is no arrangement of frequency control in the control calculation. However the speed control component of model of the diesel motor can keep up the frequency of the supply practically at 50 Hz with little

variation of $\pm 0.2\%$. Subsequently, the proposed PMSG based DG set along with STATCOM can be utilized for sustaining straight and nonlinear adjusted and unequal burdens.

The proposed PMSG based DG set has fuzzy logic controller additionally inalienable with high effectiveness. Adaline based fuzzy controller gives the better results compared to PI controller. The comparison of %THD values using PI Controller and FLC is shown in Table-2.

IX. REFERENCES

- [1]. Xibo Yuan; Fei Wang; Boroyevich, D.; Yongdong Li; Burgos, R., "DC-link Voltage Control of a Full Power Converter for Wind Generator Operating in Weak-Grid Systems," IEEE Transactions on Power Electronics, vol.24, no.9, pp.2178-2192, Sept. 2009.
- [2]. Li Shuhui, T.A. Haskew, R. P. Swatloski and W. Gathings, "Optimal and Direct-Current Vector Control of Direct-Driven PMSG Wind Turbines," IEEE Trans. Power Electronics, vol.27, no.5, pp.2325-2337, May 2012.
- [3]. M. Singh and A. Chandra, "Application of Adaptive Network-Based Fuzzy Inference System for Sensorless Control of PMSG-Based Wind Turbine With Nonlinear-Load-Compensation Capabilities," IEEE Trans. Power Electronics, vol.26, no.1, pp.165-175, Jan. 2011.
- [4]. A. Rajaei, M. Mohamadian and A. Yazdian Varjani, "Vienna-Rectifier-Based Direct Torque Control of PMSG for Wind Energy Application," IEEE Trans. Industrial Elect., vol.60, no.7, pp.2919-2929, July 2013.
- [5]. Mihai Comanescu, A. Keyhani and Dai Min, "Design and analysis of 42-V permanent-magnet generator for automotive applications," IEEE Trans. Energy Conversion, vol.18, no.1, pp.107-112, Mar 2003.
- [6]. S. Javadi and M. Mirsalim, "Design and Analysis of 42-V Coreless Axial-Flux Permanent-Magnet Generators for Automotive Applications," IEEE Trans. Magnetics, vol.46, no.4, pp.1015-1023, April 2010
- [7]. F. Crescimbeni, A. Lidozzi and L. Solero, "High-Speed Generator and Multilevel Converter for Energy Recovery in Automotive Systems," IEEE

- Trans. Industrial Elect., vol.59, no.6, pp.2678-2688, June 2012
- [8]. W.U.N. Fernando, M. Barnes, and O. Marjanovic, "Direct drive permanent magnet generator fed AC-DC active rectification and control for more-electric aircraft engines," IET Electric Power Applications, vol.5, no.1, pp.14-27, January 2011.
- [9]. A. D. Hansen and G. Michalke, "Multi-pole permanent magnet synchronous generator wind turbines' grid support capability in uninterrupted operation during grid faults," IET Renewable Power Generation, vol.3, no.3, pp.333-348, Sept. 2009.
- [10]. A. Uehara, A. Pratap, T. Goya, T. Senjyu, A. Yona, N. Urasaki and T. Funabashi, "A Coordinated Control Method to Smooth Wind Power Fluctuations of a PMSG-Based WECS," IEEE Trans. Energy Conversion, vol.26, no.2, pp.550-558, June 2011.
- [11]. T. F. Chan, LL. Lai and Yan Lie-Tong, "Performance of a three-phase AC generator with inset Nd-Fe-B permanent-magnet rotor," IEEE Trans. Energy Conversion, vol.19, no.1, pp.88-94, March 2004.
- [12]. Z. Chen, E. Spooner, W. T. Norris and A. C. Williamson, "Capacitor-assisted excitation of permanent-magnet generators," IEE Proc. Electric Power Applications, vol.145, no.6, pp.497-508, Nov 1998.
- [13]. M.A. Rahman, A. M. Osheiba, T.S. Radwan and E.S. Abdin, "Modelling and controller design of an isolated diesel engine permanent magnet synchronous generator," IEEE Trans. Energy Conversion, vol.11, no.2, pp.324-330, Jun 1996.
- [14]. Y. Errami, M. Maaroufi and M. Ouassaid, "Variable Structure Direct Torque Control and grid connected for wind energy conversion system based on the PMSG," International Conference on Complex Systems (ICCS), 2012, pp.1-6, 5-6 Nov. 2012.
- [15]. B. Singh and J. Solanki, "Load Compensation for Diesel Generator-Based Isolated Generation System Employing DSTATCOM," IEEE Trans. Industry Applications, vol.47, no.1, pp.238-244, Jan.-Feb. 2011.
- [16]. P. Mitra and G.K. Venayagamoorthy, "An Adaptive Control Strategy for DSTATCOM Applications in an Electric Ship Power System," IEEE Trans. Power Electronics, vol.25, no.1, pp.95-104, Jan. 2010.
- [17]. A. Ghosh and G. Ledwich, "Load compensating DSTATCOM in weak AC systems," IEEE Trans. Power Delivery, vol.18, no.4, pp.1302-1309, Oct. 2003
- [18]. B. Singh and S.R. Arya, "Adaptive Theory-Based Improved Linear Sinusoidal Tracer Control Algorithm for DSTATCOM," IEEE Trans. Power Electronics, vol.28, no.8, pp.3768-3778, Aug. 2013.
- [19]. B. Singh and S. Sharma, "Stand-Alone Single-Phase Power Generation Employing a Three-Phase Isolated Asynchronous Generator," IEEE Trans. Industry Applns., vol.48, no.6, pp.2414-2423, Nov.-Dec. 2012.
- [20]. B. Singh, V. Sheeja, R. Uma and P. Jayaprakash, "Voltage- frequency controller for standalone WECS employing permanent magnet synchronous generator," International Conference on Power Systems, 2009. ICPS '09, pp.1-6, 27-29 Dec. 2009.
- [21]. B. Singh, S.R. Arya, A. Chandra and K. Al-Haddad, "Implementation of adaptive filter based control algorithm for Distribution Static Compensator," Annual Meeting Industry Applications Society (IAS), 2012 IEEE, pp.1-8, 7-11 Oct. 2012.
- [22]. B. Singh and J. Solanki, "A comparison of control algorithms for DSTATCOM," IEEE Trans. Ind. Elect., vol.56, no.7, pp.2738-2745, July 2009.
- [23]. Bhim Singh, Ram Nivas, IEEE Transactions on Industry Applications, Volume: 52, Issue: 1, Jan.-Feb. 2016.